Containment Pressure

Model for Maine Yankee ECCS

Performance Evaluation

by

P. J. Guimond

Nuclear Engineering Department

November 1978

Prepared By Philip J. Guimond — Feb 16, 1979 (Date)

Reviewed By [signature] — Feb 20, 1979 (Date)

Approved By [signature] — 2-27-79 (Date)

Yankee Atomic Electric Company
Nuclear Services Division
20 Turnpike Road
Westborough, Massachusetts 01581

7903270556

DISCLAIMER OF RESPONSIBILITY

This document was prepared by Yankee Atomic Electric Company on behalf of Maine Yankee Atomic Power Company. This document is believed to be completely true and accurate to the best of our knowledge and information. It is authorized for use specifically by Yankee Atomic Electric Company, Maine Yankee Atomic Power Company and/or the appropriate subdivisions within the Nuclear Regulatory Commission only.

With regard to any unauthorized use whatsoever, Yankee Atomic Electric Company, Maine Yankee Atomic Power Company and their officers, directors, agents and employees assume no liability nor make any warranty or representation with respect to the contents of this document or to its accuracy or completeness.

ABSTRACT

An analytical model for predicting the minimum containment pressure of the Maine Yankee Atomic Power Station following a loss-of-coolant accident (LOCA) is presented in this report. The model uses the CONTEMPT-LT Version 26 computer program (Containment Temperature Pressure Transient - Long Term) developed by Aerojet Nuclear Company for ERDA.

The minimum containment pressure prediction is used as an input to the ECCS performance evaluation model of the Maine Yankee Atomic Power Station. A benchmark analysis of the containment pressure response following a postulated LOCA at Maine Yankee agrees well with results predicted by Combustion Engineering, Inc.

TABLE OF CONTENTS

LIST OF FIGURES

LIST OF TABLES

ACKNOWLEDGEMENTS

The author wishes to thank A.E. Ladieu and R.N. Henault for their technical advice and assistance.

1.0 INTRODUCTION

Following a loss-of-coolant accident at Maine Yankee, the emergency core cooling system (ECCS) will supply water to the reactor vessel to reflood and cool the reactor core. The rate of core reflooding is governed by the capability of the ECCS water to displace steam generated in the reactor vessel during the core reflooding period. For PWR plants like Maine Yankee, there is a direct dependence of core flooding rate on containment pressure, i.e. the core flooding rate will increase with increasing containment pressure. Therefore as part of the overall evaluation of ECCS performance, paragraph I.D.2 of Appendix K to 10 CFR Part 50 requires that the containment pressure used in the evaluation of the performance capability of a PWR ECCS not exceed a pressure calculated conservatively for that purpose. The following guidelines are provided in the USNRC Standard Review Plan 6.2.1.5 (Reference 1) and indicate the conservatism that is required in analyzing the minimum containment pressure response to a LOCA for use in ECCS performance capability.

1. Mass and energy release data should be determined in accordance with 10 CFR Part 50 Appendix K, requirements.

2. Containment structure modelling should be in compliance with recommendations given in Branch Technical Position CSB6-1 "Minimum Containment Pressure Model for PWR ECCS Performance Evaluation" (Reference 2).

This report describes the analytical model used by Yankee to predict a conservatively low containment pressure response to a LOCA at Maine Yankee for use in conjunction with Yankee's ECCS performance model of the Maine Yankee Atomic Power Station (References 3 & 4).

The model utilizes the CONTEMPT-LT Version 26 (Containment Temperature - Pressure Transient-Long Term) computer program developed by Aerojet Nuclear Company for the Energy Research and Development Admi ation (References 5,6 and 7).

Model benchmarking was accomplished by direct comparison of predicted containment pressure response to a DECLG (Double-Ended Cold Leg Guillotine) LOCA event at Maine Yankee to previously reported results of an analysis of the same event by Combustion Engineering for the Cycle 3 reload submittal (References 8 & 9). Results show reasonable agreement between the two predictions with the YAEC CONTEMPT-LT/026 model producing a slightly more conservative response.

2.0 MODEL DESCRIPTION

The analytical model of the Maine Yankee containment volume consists of two regions: a gas region at the top containing a steam-air mixture and a liquid region at the bottom containing the sump water. The steam-air mixture is assumed to be in thermal equilibrium. This does not imply thermal equilibrium between the steam-air mixture and the water region. The liquid region is assumed to be at the total containment pressure, and may be at a different temperature than the vapor region.

Prior to the initiation of blowdown, the containment system is assumed to be in a steady state condition. From the steady state condition, the partial pressure, masses, and energy contents of the different components and the temperature distribution through the heat conducting structures are computed. These values are used as the initial conditions for the transient.

The transient phase starts with the rupture of the reactor coolant pipe. The discharge flow at the break area separates into steam and water phases, depending on the containment total pressure and the energy content of the blowdown. The part flashing to steam is added to the gas region while the liquid portion enters the containment sump.

In the analysis a quasi-steady condition is assumed during any small time interval, and an equilibrium solution is obtained through a mass and energy balance with proper consideration for heat-conduction to the structures. The heat structures may conduct heat from either the liquid or the vapor region. The liquid region can be at subcooled or saturated conditions corresponding to the total containment pressure; while steam in the vapor region can exist at saturated or superheated conditions corresponding to the partial pressure of steam. Air and steam are assumed to be at the same teperature. Boiling of the liquid and condensation of the vapor are taken into account in the mass and energy balance.

The thermodynamic properties of steam and water are computed using the STH 20 Subroutines (Reference 7). Air is treated as an ideal gas; homogeneous mixing of the steam-air mixture is assumed.

The containment building is divided into a number of heat-conducting sections. Heat-conducting sections are also used to describe building internals which act as heat sinks such as piping or reactor vessel components.

Every heat conducting section is treated as a one-dimensional slab, subdivided into a number of nodes to represent thickness. An energy conservation equation, expressed in finite difference form accounts for transient conduction into and out of each node and the temperature rise of the node.

The heat transfer at a boundary is equal to the heat-transfer coefficient times the difference between the surface temperature and a bulk fluid temperature. The heat-transfer coefficients used are discussed in Section 3.5.

3.0 INPUT DATA

3.1 Initial Conditions

The initial internal containment conditions are listed in Table 3.1. The minimum containment atmospheric temperature and pressure, and the maximum humidity encountered under limiting normal operating conditions were used in compliance with BTP CSB 6-1 recommendations. The ambient temperature external to the containment was assumed to be -20 F.

3.2 Containment Volume Data

The maximum containment net free volume including uncertainties was used and is given in Table 3.1 This value was calculated by Stone and Webster Corporation and reported in Reference 10. The maximum gross containment volume (including uncertainty) minus the minimum volumes (including uncertainties) of the individual internal structures was used in the determination of this value.

3.3 Mass and Energy Addition Data

Mass and energy release to the containment will be calculated in accordance with 10 CFR Part 50 Appendix K (Reference 11) using the YAEC Maine Yankee ECCS performance model (References 3,4). All primary coolant blowdown (from both ends of double ended breaks), direct spillage of accumulator flow to containment, and subcooled ECCS safety injection water spillage out the break will be accounted for.

3.4 Heat Conducting Structures (Passive Heat Removal)

A summary of mass and heat transfer area of the structural heat sinks is included in Table 3.1. Table 3.2 lists the same data for the individual heat slabs which are modeled in CONTEMPT. With four exceptions, all heat conducting structures are modeled as symmetrical slabs exposed on both sides to the containment vapor space. Thus, the exposed surface areas shown in Table 3.2 for these slabs is the total for both sides and the thickness shown is the half-thickness. The exceptions are slabs 16, 17, 18 and 20 which represent the containment shell and dome and the floor. These are modeled as full thickness heat slabs with one side of the shell and dome exposed to the external environment and the other to the internal vapor space, and one side of the floor slab exposed to the pool or sump water and the other to the earth. The areas listed in Table 3.2 for these heat slabs are the single-sided area and the thickness shown is the full thickness.

The effect of paint on heat transfer rate is considerable and for LOCA/ECCS calculations it is conservative to neglect the existence of the paint layer on all painted surfaces, thereby increasing the heat sink effectiveness during the early portion of the transient. Similarly, zinc coatings on galvanized steel are also neglected.

Table 3.3 lists the thermophysical properties used in the model.

Table 3.4 lists the mesh spacing used in each material to model the heat conducting structures.

3.5 Heat Transfer Coefficients

Three different classes of heat transfer surface are inherent in the model. Surfaces exposed to the containment vapor space, surfaces exposed to the sump and pool liquid, and external surfaces exposed to the environment. Each type of surface is treated in a different manner.

3.5.1 Surfaces Exposed to the Container Vapor Space

The heat transfer coefficient used for this class of surfaces during the different phases of a LOCA are described below. These are the same as those prescribed in Reference 2, Branch Technical Position CSB 6-1, and are based upon the work of Tagami (Reference 14) and Uchida (Reference 12).

(1) During the blowdown phase, h_s was assumed to follow a linear increase in the condensing heat transfer coefficient from $h_{initial}$=8 Btu/hr-ft^2-^oF, at t = 0, to a peak value four times greater than the maximum calculated condensing heat transfer coefficient at the end of blowdown, using the Tagami correlation, (Reference 2).

$$h_{max} = 4 \times h_{Tagami} = 4 \times [72.5 \times [Q/Vt_p]^{0.62}]$$

where h_{max} = maximum heat transfer coefficient, Btu/hr-ft^2-^oF

Q = primary coolant energy, Btu

V = net free containment volume, ft^3

t_p = time interval to end of blowdown, sec.

h_s = surface heat transfer coefficient, Btu/hr-ft^2-^{o}F.

(2) During the long-term post-blowdown phase of the accident, characterized by low turbulence in the containment atmosphere, a condensing heat transfer coefficient 1.2 times greater than those predicted by the Uchida data (Reference 12) and given in Table 3.5 was used.

(3) During the transition phase of the accident, between the end of blowdown and the long-term post-blowdown phase, a conservative exponential transition in the condensing heat transfer coefficient was calculated as shown in Figure 3.1.

The calculated condensing heat transfer coefficient based on the above method was applied to all exposed passive heat sinks, both metal and concrete.

Heat transfer between adjoining materials in the passive heat absorbing structures was based on the assumption of no resistance to heat flow at the material interfaces.

3.5.2 Surfaces Exposed to the Liquid Region

A heat transfer coefficient of 500 Btu/hr-ft^2-^{o}F was used between the liquid region pool and heat transfer surfaces in contact with it, namely the floor slab and sump. This is consistent with the value previously used by CE for the Cycle 3 and Cycle 4 analyses. (References 8, 9).

3.5.3 Surfaces Exposed to the External Environment

Heat conducting structures such as the containment shell and dome are exposed on one side to the ambient atmosphere. The natural convection heat transfer coefficient assumed for these surfaces is 2.0 Btu/hr-ft^2-^{o}F consistent with the value used by CE in the Cycle 3 and Cycle 4 analyses. (References 8, 9). Sensitivity studies show that containment pressure is not sensitive to this value over the time span of interest.

3.6 Active Heat Removal Systems

All active heat removal systems which function to control or limit the containment pressure or temperature following a LOCA are assumed to be operable in the model at their maximum heat removal capacities.

3.6.1 Containment Spray System

For the purposes of this model both containment spray pumps are assumed to actuate at time zero following the LOCA and are assumed to deliver their maximum flow capacity of 4000 gpm per pump to the containment spray headers. The temperature of the containment spray water is assumed to be 40 F, the minimum temperature allowed by the Maine Yankee Technical Specifications for the stored spray water. Spray "effectiveness" is assumed to be 100%.

3.6.2 Recirculation Fan Coolers

The six air recirculation fan coolers are not of engineered safety feature grade, however, they are all assumed to be operating at time zero, and to remain operable throughout the transient, with heat removal capacity given in Table 3.6.

3.6.3 Subcooled ECCS Spillage

The spillage of subcooled ECCS water into the containment and subsequent steam-water mixing is taken into consideration by multiplying the ECCS spillage flow rate by a correction factor which accounts for its higher enthalpy (and hence lower spray efficiency). The corrected spillage flow rate is, in turn added to the containment spray flow rate assuming it to be at the same temperature and enthalpy as the spray flow.

3.7 Time Steps

Time step values were selected so that small time steps were used during periods of high rates of change of containment conditions. Larger time steps were used when containment conditions were changing slowly. The convergence parameter, dE/E, edited by CONTEMPT was kept at or below 0.1% as recommended on page 200 of Reference 5. This criterion was verified as being adequate to guarantee a converged solution by reducing the time step size by a factor of 20 for the first 100 seconds with no observed change in results. The time steps used are shown in Table 3.7.

3.8 Methodology

In order to run CONTEMPT-LT/026 in its present version in compliance with CSB6.1, heat transfer coefficient requirements, it is necessary to make two separate computer runs.

The first run is made with the heat sink boundary condition option set equal to -5 on all containment internal surfaces except the floor slabs. This allows the user to input in a table the initial values for h_{cond} during the blowdown period from h=8.0 (BTU/hr-ft^2-^{o}F) to h=4 x h_{Tagami}. When the code detects end-of-blowdown on the 300 series Mass + Energy input, the values used for h_{cond} on these internal surfaces is calculated by CONTEMPT-LT to be equal to h_{Uchida}. This provides a good first approximation of the air/water mass ratios during the transition period and a set of initial estimates of h_{Uchida} to be used in calculating values of h_{stag} in compliance with CSB 6.1 for the transition period following end of blowdown. These are calculated by the user and input to CONTEMPT-LT as a heat transfer coefficient versus time table for the second computer run.

The second computer run is made with identical input as the first with the exception of the internal heat slabs boundary condition options being set equal to +5, which forces CONTEMPT to use the input table of heat transfer coefficient versus time calculated by the user to be in conformance with CSB 6.1.

This two-step method will be required until CONTEMPT-LT/026 can be modified to internally calculate transition period values of the heat transfer coefficient and reflect the 1.2 x h_{Uchida} constant factor called for by Branch Technical Position CSB 6.1.

This two-step approach results in slightly more conservative (i.e., high) values for h_{cond} than an integral calculation would predict. This is attributable to the use of the value for h_{Uchida} calculated by CONTEMPT-LT in the first run as the first approximation for h_{stag} in the equation used to calculate the transition values for h_{cond} given on Figure .5. The values of h_{Uchida} calculated in the first run are based on air/steam mass ratios which are lower than would be predicted using the appropriate CSB 6.1 value for h_{cond} (i.e., at a given point in time after blowdown more steam would have been condensed if a heat transfer coefficient complying with CSB 6.1 had been used). Thus, the values for h_{stag} are high and the values input to the second computer run for h_{cond} after the end-of-blowdown are also slightly conservative.

4.0 SAMPLE PROBLEM

The sample problem analyzed was the containment pressure following a postulated DECLG (Double-Ended Cold Leg Guillotine) break at Maine Yankee. This transient was analyzed by Combustion Engineering for the Maine Yankee ECCS performance reload analysis for Cycles 3 and 4 (References 11,12). Mass and energy release data, Table 4.1, for this event reported by CE in Reference 8 was input to the CONTEMPT-LT model of the Maine Yankee containment described in Section 2.0 and 3.0 of this report. Comparison of the resulting minimum containment pressure prediction to the corrected CE prediction reported in Reference 9 shows excellent agreement (Figure 4.1).

5.0 REFERENCES

1. USNRC Standard Review Plan 6.2.15 Minimum Containment Pressure Analysis for Emergency Core Cooling System Performance Capability Studies, (March, 1975).

2. USNRC, Branch Technical Position CSB 6-1, "Minimum Containment Pressure Model for PWR ECCS Performance Evaluation", Part of Standard Review Plan 6.2.15, (March, 1975).

3. A. Husain et al., Application of Yankee-WREM-Based Generic PWR ECCS Evaluation Model to Maine Yankee (3-Loop Sample Problem), YAEC-1160 (July, 1978).

4. A. Husain et al., Application of Yankee-WREM-Based Generic PWR ECCS Evaluation Model to Maine Yankee (2-Loop Sample Problem) Break in Active Loop, YAEC-1164 (September, 1978).

5. L.L. Wheat, et al., CONTEMPT-LT: A Computer Program for Predicting Containment Pressure-Temperature Response to a Loss-of-Coolant Accident, ANCR-1219, (June, 1975).

6. W.J. Mings, Version 26 Modifications to the CONTEMPT-LT Program, SRD-83-76, INEL (April, 1976).

7. R.J. Wagner, STH2O, A Subroutine Package to Compute the Thermodynamic Properties of Water, Aerojet Nuclear Company (April 30, 1975).

8. MYAPCo letter to NRC WMY77-3 dated January 12, 1977, Proposed Change

#52-Cycle 3 Reload Supplement No. 1.

9. CE Letter to MYAPCo, "Maine Yankee Core IV ECCS Performance Results", CE 3068-075, (June 23, 1978).

10. Stone and Webster Engineering Corporation letter to MYAPCo, dated May 14, 1976, Attachment 1, "Containment Data Maine Yankee Nuclear Plant".

11. 10 CFR Part 50.46, "Acceptance Criteria for Emergency Core Cooling Systems for Light Water Nuclear Power Reactors", and 10 CFR Part 50, Appendix K, "ECCS Evaluation Models".

12. H. Uchida, A. Oyama, and Y. Toga, "Evaluation of Post-Incident Cooling Systems of Light-Water Power Reactors", Proc. Third International Conference on the Peaceful Uses of Atomic Energy, Volume 13, Session 3.9, United Nations, Geneva (1964).

13. R. Byron Bird, et al., Transport Phenomena, John Wiley & Sons, Inc., p. 353, (1960).

14. T. Tagami, "Interim Report on Safety Assessments and Facilities Establishment Project in Japan for Period Ending June 1965 (No. 1)," prepared for the National Reactor Testing Station, February 28, 1966 (unpublished work).

Figure 3.1

Condensing Heat Transfer Coefficients for Heat Absorbing Surfaces

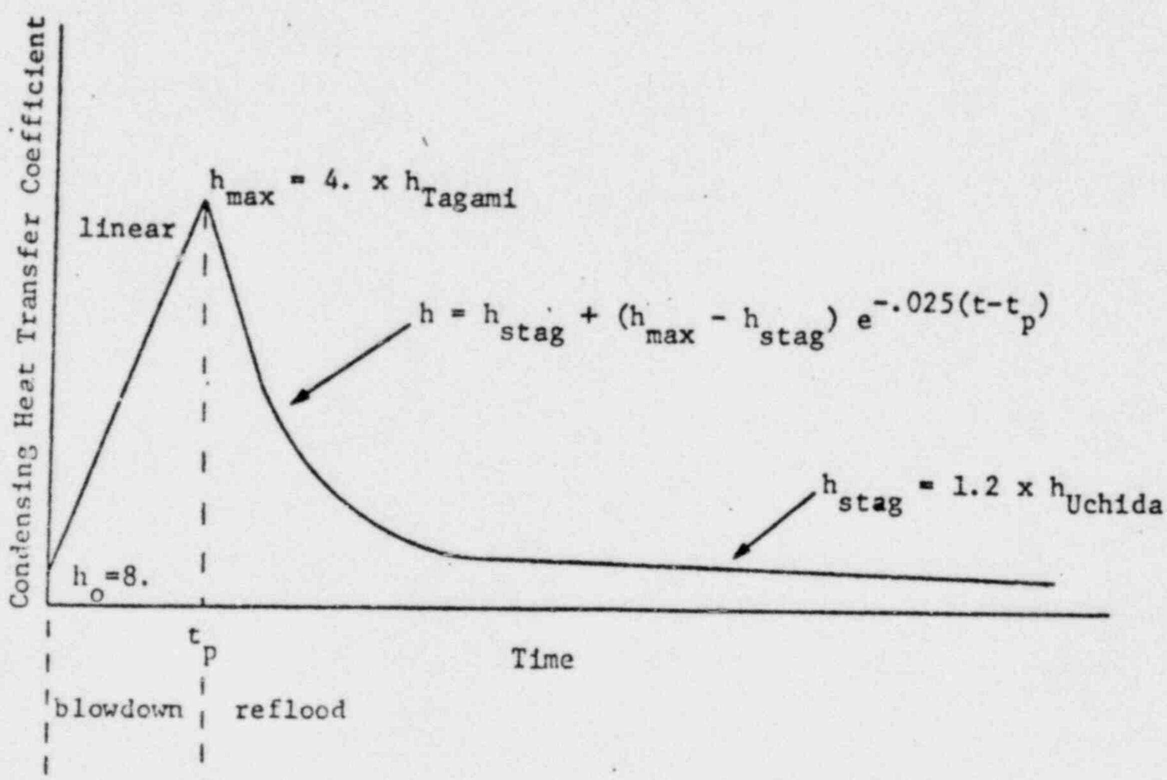

FIGURE 4.1

MAINE YANKEE CORE 4

0.5 x DOUBLE ENDED GUILLOTINE BREAK IN PUMP DISCHARGE LEG

CONTAINMENT PRESSURE

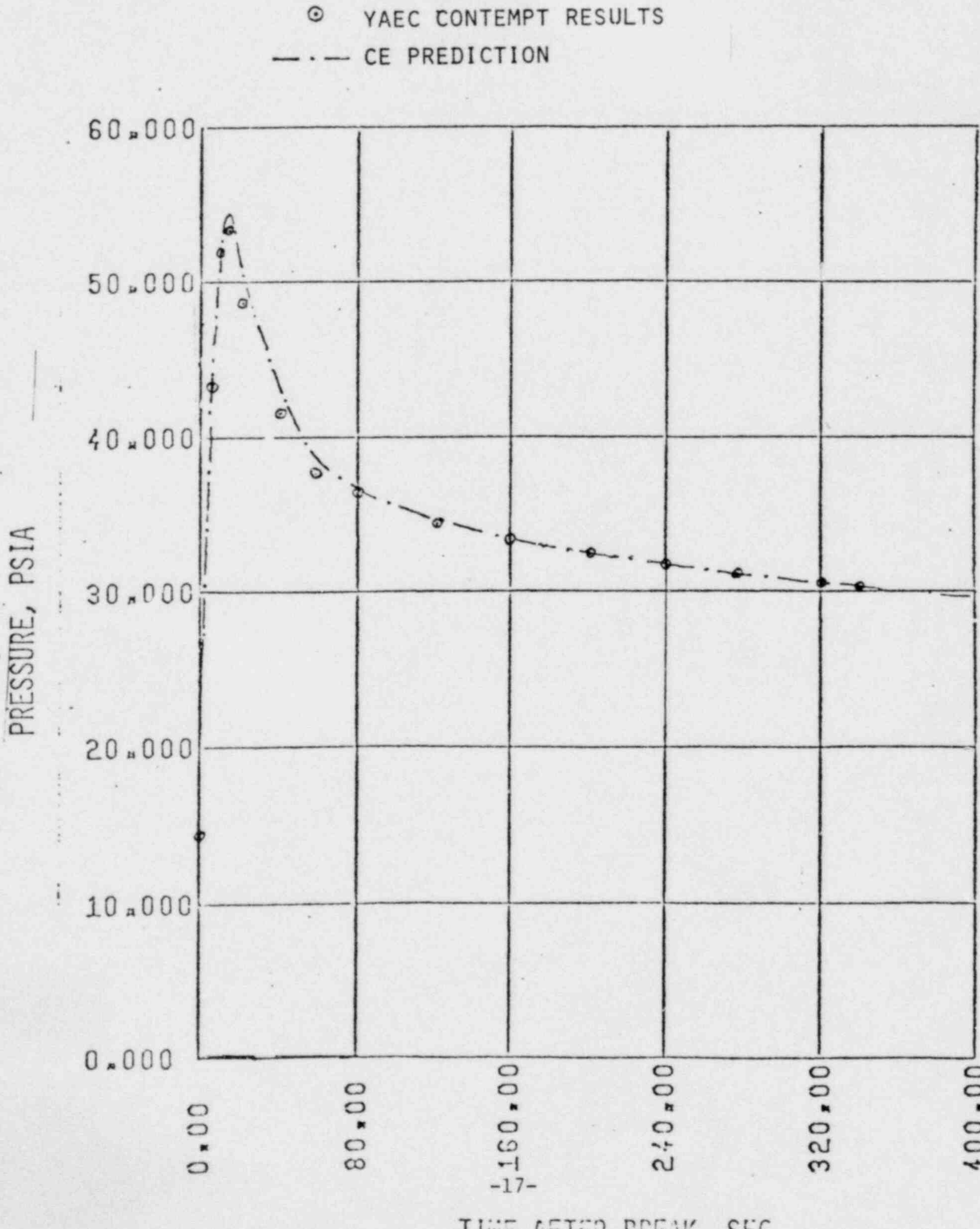

TABLE 3.1

Containment Data for ECCS Evaluation Model

Net Free Volume	1.842×10^6 ft^3
Initial Conditions	
Internal Pressure	14.7 psia
Internal Temperature	60 F
Relative Humidity	100%
External Air Temperature	-20 F
RWST Temperature	40 F
Spray System	
Number of Trains Operating	2
Spray Flow Rate Per Train	4000 gpm
Assumed Actuation Time	0
Assumed Delay Time	0
Recirculation Fan Coolers	
Number of Fan Coolers Operating	6
Heat Removal Capacity	Table
Heat Sinks	
Misc. Steel Heat Sinks	208,195 ft^2 2.43×10^6 LBM
Lined Concrete Heat Sinks	57,600 ft^2 1.04×10^6 LBM (STEEL)
Unlined Concrete Heat Sinks	119,997 ft^2

Table 3.2

Containment Heat Absorbing Surfaces

Slab No.	Description	Material	Thickness, Inches	Heat Sink Area, ft^2
1	Structural Steel & Refueling Cavity Liner	Carbon Steel	0.12	75465
2	Misc. Steel	Carbon Steel	0.436	9183
3	Misc. Steel	Carbon Steel	1.23	12556
4	Misc. Steel	Carbon Steel	0.273	36339
5	Misc. Steel	Carbon Steel	0.843	7779
6	Equip. and Supports	Carbon Steel	2.40	480
7	Equip. and Supports	Carbon Steel	7.73	1593
8	Equip. and Personnel Hatch Flanges	Carbon Steel	4.84	65
9	Equipment, Piping	Stainless Steel	0.149	391
10	Misc. Piping	Stainless Steel	0.40	5585
11	Cable Trays, Conduit, Duct Work	Galvanized Steel	.037	60873
12	Conduit	Galvanized Steel	0.23	4609
13	Internal Walls and Floors	Concrete	0.94 ft	66681
14	Internal Walls and Floors	Concrete	1.47 ft	48619
15	Internal Walls and Floors	Concrete	4.07 ft	9593
16	Containment Dome	Carbon Steel Concrete	0.5 2 ft 6 in	28862
17	Containment Dome Vent	Carbon Steel Concrete	3.0 2.5 ft	4
18	Containment Shell	Carbon Steel Concrete	0.384 4.5 ft	29601

Table 3.2 (cont.)

Slab No.	Description	Material	Thickness, Inches	Heat Sink Area, ft^2
19	Steam Generator Supports	Carbon Steel	0.5	246
		Concrete	6.5 ft	
20	Floor Slab	Concrete	24.0	11830
		Carbon Steel	0.375	
		Concrete	120.0	

Table 3.3

Thermophysical Properties

Material	Conductivity (BTU/Hr-Ft-^{o}F)	Volume Heat Capacity (BTU/Ft^{3} - ^{o}F)
Carbon Steel	30.	60.
Stainless Steel	10.	60.
Concrete	1.5	32.

Table 3.4

Heat Structure Material Mesh Spacing

Material	Mesh Sizes, Inches
Stainless Steel	.037/.040*
Carbon Steel	.030/.050*
Concrete[1]	0.1

* Minimum/Maximum mesh spacing used.

[1] First four inches only, this corresponds to the thermal penetration thickness[2] in concrete for the time span of interest. Mesh size beyond four inches confirms with recommendations made on P35 of Reference 5.

[2] Distance within a semi-infinite uniform slab beyond which temperature changes less than 1% of a step change occurring at the slab boundary surface. (Reference 13)

Table 3.5

UCHIDA Heat Transfer Coefficients

Mass Ratio (lb air/lb steam)	Heat Transfer Coefficient (Btu/hr-ft^2-^{o}F	Mass Ratio (lb air/lb steam)	Heat Transfer Coefficient (Btu/hr-ft^2-^{o}F)
50	2	3	29
20	8	2.3	37
18	9	1.8	46
14	10	1.3	63
10	14	0.8	98
7	17	0.5	140
5	21	0.1	280
4	24		

Table 3.6

Fan Coolers Heat Removal Capacity

Vapcr Temperature, (^{o}F)	Capacity, (Btu/Hr)
90.0	0.0
200.	79.873×10^{6}
300.0	152.484×10^{6}

Table 3.7

Time Step Used for 1.0 DECLG
LOCA Sample Problem

Time Interval, (seconds)	Time Step, (seconds)
0.0 - 20.0	0.01
20.0 - 40.0	0.05
40.0 - 100.0	0.10
100.0 - 400.0	0.50

TABLE 4.1

Maine Yankee Core III
Blowdown and Reflood Mass and Energy Release DAta
1.0 DEG/PD

Time Sec	Mass Flow lbm/sec	Energy Release Btu/sec	Integral of Mass Flow lbm	Integral of Energy Release Btu
0.0	0.0	0.0	0.0	0.0
0.05	8.246×10^4	4.505×10^7	4.2614×10^3	2.3272×10^6
0.10	9.027×10^4	4.935×10^7	8.5023×10^3	4.6465×10^6
0.15	9.031×10^4	4.933×10^7	1.3016×10^4	7.1125×10^6
0.20	8.741×10^4	4.778×10^7	1.7422×10^4	9.5193×10^6
0.25	8.684×10^4	4.753×10^7	2.1785×10^4	1.1906×10^7
0.35	8.454×10^4	4.634×10^7	3.0371×10^4	1.6609×10^7
0.45	8.396×10^4	4.606×10^7	3.8813×10^4	2.1239×10^7
0.60	8.314×10^4	4.564×10^7	5.1370×10^4	2.8130×10^7
0.80	8.287×10^4	4.555×10^7	6.7964×10^4	3.7245×10^7
1.0	8.143×10^4	4.483×10^7	8.4384×10^5	4.6278×10^7
1.2	7.851×10^4	4.330×10^7	1.0039×10^5	5.5101×10^7
1.4	7.355×10^4	4.063×10^7	1.1559×10^5	6.3488×10^7
1.6	6.975×10^4	3.859×10^7	1.2990×10^5	7.1397×10^7
1.8	6.697×10^4	3.710×10^7	1.4361×10^5	7.8990×10^7
2.0	6.248×10^4	3.464×10^7	1.5655×10^5	8.6157×10^7
2.4	5.576×10^4	3.097×10^7	1.8013×10^5	9.9242×10^7
2.8	5.156×10^4	2.868×10^7	2.0152×10^5	1.1113×10^8
3.2	4.852×10^4	2.405×10^7	2.2152×10^5	1.2227×10^8
3.6	4.621×10^4	2.584×10^7	2.4041×10^5	1.3282×10^8
4.0	4.404×10^4	2.475×10^7	2.5848×10^5	1.4295×10^8
4.8	3.959×10^4	2.265×10^7	2.9200×10^5	1.6193×10^8
5.6	3.577×10^4	2.087×10^7	3.2203×10^5	1.7929×10^8
6.4	3.231×10^4	1.927×10^7	3.4935×10^5	1.953[illegible] $\times 10^8$
7.2	2.807×10^4	1.733×10^7	3.7349×10^5	2.1002×10^8
8.0	2.274×10^4	1.520×10^7	3.9399×10^5	2.2306×10^8
8.8	1.488×10^4	1.275×10^7	4.0891×10^5	2.3420×10^8
9.6	1.267×10^4	1.117×10^7	4.1966×10^5	2.4360×10^8
10.5	9.425×10^3	9.570×10^6	4.2955×10^5	2.5302×10^8
11.5	7.164×10^3	8.023×10^6	4.3777×10^5	2.6178×10^8
12.5	5.444×10^3	6.473×10^6	4.4408×10^5	2.6906×10^8
13.5	3.541×10^3	4.366×10^6	4.4857×10^5	2.7451×10^8
14.5	2.029×10^3	2.556×10^6	4.5130×10^5	2.7791×10^8
15.5	9.390×10^2	1.172×10^6	4.5273×10^5	2.7971×10^8
16.5	5.704×10^1	6.662×10^4	4.5316×10^5	2.8022×10^8
17.4	7.115×10^2	8.903×10^5	4.5325×10^5	2.8032×10^8
	Time of Annulus Downflow			
	Start of Reflood (Values Below are for Steam Only)			
30.84	0.0	0.0	4.5325×10^5	2.8032×10^8
40.84	0.0	0.0	4.5325×10^5	2.8032×10^8
50.84	0.0	0.0	4.5325×10^5	2.8032×10^8

TABLE 4.1
(Continued)

Time Sec	Mass Flow lbm/sec	Energy Release Btu/sec	Integral of Mass Flow lbm	Integral of Energy Release Btu
60.84	1.9313×10^2	2.5208×10^5	4.5483×10^5	2.8239×10^8
70.84	2.1843×10^2	2.8509×10^5	4.5672×10^5	2.8485×10^8
80.84	2.1060×10^2	2.7488×10^5	4.5885×10^5	2.8763×10^8
90.84	2.0663×10^2	2.6970×10^5	4.6094×10^5	2.9036×10^8
100.84	2.0250×10^2	2.6430×10^5	4.6299×10^5	2.9303×10^8
120.84	1.9645×10^2	2.5641×10^5	4.6697×10^5	2.9822×10^8
140.84	1.9153×10^2	2.4998×10^5	4.7084×10^5	3.0328×10^8
160.84	1.8898×10^2	2.4665×10^5	4.7464×10^5	3.0824×10^8
180.84	1.8658×10^2	2.4353×10^5	4.7839×10^5	3.1314×10^8
200.84	1.8524×10^2	2.4178×10^5	4.8212×10^5	3.1800×10^8
220.84	1.8581×10^2	2.4252×10^5	4.8583×10^5	3.2285×10^8
240.84	1.8536×10^2	2.4193×10^5	4.8955×10^5	3.2769×10^8
260.84	1.8606×10^2	2.4284×10^5	4.9326×10^5	3.3254×10^8
280.84	1.8626×10^2	2.4311×10^5	4.9698×10^5	3.3740×10^8
300.84	1.8704×10^2	2.4412×10^5	5.0071×10^5	3.4226×10^8
320.84	1.8632×10^2	2.4319×10^5	5.0444×10^5	3.4714×10^8
340.84	1.8644×10^2	2.4334×10^5	5.0818×10^5	3.5201×10^8
360.84	1.8669×10^2	2.4367×10^5	5.1191×10^5	3.5689×10^8
380.84	1.8758×10^2	2.4483×10^5	5.1565×10^5	3.6117×10^8
400.84	1.8721×10^2	2.4435×10^5	5.1940×10^5	3.6665×10^8
430.84	1.8723×10^2	2.4438×10^5	5.2502×10^5	3.7399×10^8